Reflectometry of drying paint

N J Elton, Surfoptic Ltd
A Legrix, Imerys Minerals Ltd

Summary

This note describes the use of the Imaging Reflectometer for studying the drying of paint. Measurements of gloss, refractive index and microroughness show how surface structure evolves as a function of time. Measurements of backscatter intensity are used to assess corresponding changes in the bulk of the paint film. The drying behaviour of model paints formulated at different PVC levels (below, at and above the CPVC) is compared.

1. Introduction

Various authors have studied the structure and gloss of drying paint films. Braun (1991) gives a comprehensive discussion and introduces the idea of a "surface critical point" marking the boundary between the film having a smooth surface stretched by surface tension in the liquid phase, and the onset of surface distortion caused by pigment particles as the drying film shrinks. Gate and Preston (1995) present an example of direct measuring of refractive index during drying of emulsion paint films using a goniophotometer. Al-Turaif and Lepoutre (2000) report a detailed study using gloss and transmittance measurements and SEM imaging of freeze-dried coatings at intermediate drying stages. Generic gloss and transmittance curves (based upon those in the literature) are shown in figure 1. Al-Turaif and Lepoutre identified two critical concentrations during the drying process, denoted the first and second critical concentration (FCC and SCC respectively).

The rise in gloss up to the FCC is attributed to an increase in refractive index as water evaporates and the concentration of pigment and binder (with relatively higher refractive index) increases. The FCC marks the formation of menisci at the surface leading to a rapid drop in gloss. Transmittance increases up to the SCC owing to a reduction in scattering efficiency due to particle crowding. The decrease in transmittance beyond the SCC is due to air replacing water in the coating layer. The SCC does not necessarily coincide with the minimum in the gloss curve. It is clear that even simple gloss curves provide considerable information about the consolidation and drying process. This note examines the additional information provided by direct measurement of refractive index and microroughness and confirms the conclusions inferred from gloss measurements.

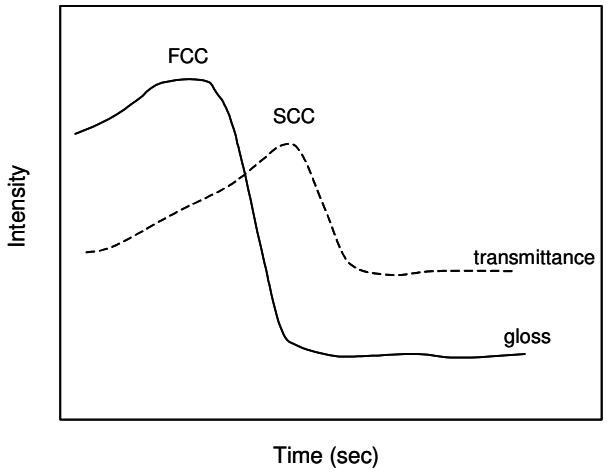

Figure 1. Generic gloss and transmittance curves for a pigmented coating near or above the CPVC. After Braun (1991), Gate and Preston (1995) and Al-Turaif and Lepoutre (2000).

2. Experimental

Paint samples were prepared by Imerys Minerals Ltd as a standard laboratory formulation based on titanium dioxide and calcined kaolin pigments in a vinyl acetate ethylene binder, but with no mineral extenders. Details of the formulation are given in Appendix I. The kaolin-binder ratio was varied to create paints covering the range of pigment volume concentrations (PVC) 20% – 55% at 5% intervals. For the drying experiments, paints at 25, 45 and 55 % PVC were selected from the series, representing films formulated below, at and above the CPVC respectively.

The paints were applied to a smooth polyester film substrate using a hand drawdown bar to give coatings at a nominal wet thickness of 50 µm. Samples were transferred immediately to the Imaging Reflectomer and a time-resolved run started, making measurements at 30s intervals over the course of 6 – 7 hours using the large measurement spot which covers an elliptical area on the sample with major axes approximately 12 x 3 mm. The typical delay between applying the film and starting the measurement was about 45s, but the films were very slow drying (typically 2 – 3hours), so this delay was negligible. Temperature and humidity in the laboratory were not controlled, but were monitored throughout the experiments. For all three drying sequences the conditions were: temperature 21 ± 1°C and relative humidity 65 ± 5%.

The x-y stage with vacuum platform was used for sample presentation. The stage height and position were pre-set using a sample of dry paint, so that wet paints could be transferred and measurements started with minimum delay. Great care was taken to protect the vacuum platform from wet paint by ensuring substrates had a generous border of unpainted area.

The usual reflectometer parameters were measured, namely refractive index, gloss (3° and 20° acceptance angles), microroughness (roughness at a scale smaller than the wavelength of light). (Macroroughness was measured by default, but not used because the substrates are macro-smooth and reflection essentially specular). Backscatter intensity was also measured – this parameter is not a standard Reflectometer output, but can readily be made available through one of the more detailed file-save options. It records intensity (expressed as photovolts) in the plane of incidence, measured over an angular acceptance of 7°, at a receiving angle of -20°.

3. Results

3.1 Measured Gloss

Figure 2 shows the data for gloss versus time for three paint formulations. The Relflectometer measures gloss at two acceptance angles, nominally 3° (G3) and 20° (G20) in the instrument used for this work. The shapes of the curves are significantly different for the two acceptance angles. The initial rise in G3 gloss for these paints is not as pronounced as that observed by Al-Turaif and Lepoutre (2000) and the time of the FCC is not clearly defined. The gloss rise and location of the FCC is more obvious for G20. The paint formulated at the CPVC immobilises fastest, while that well below the CPVC is significantly slower. The drying time is expected to depend on film thickness and the absolute time of the FCC should be treated cautiously because variations in pressure and speed of the hand drawdown mean that film thickness was not controlled very precisely.

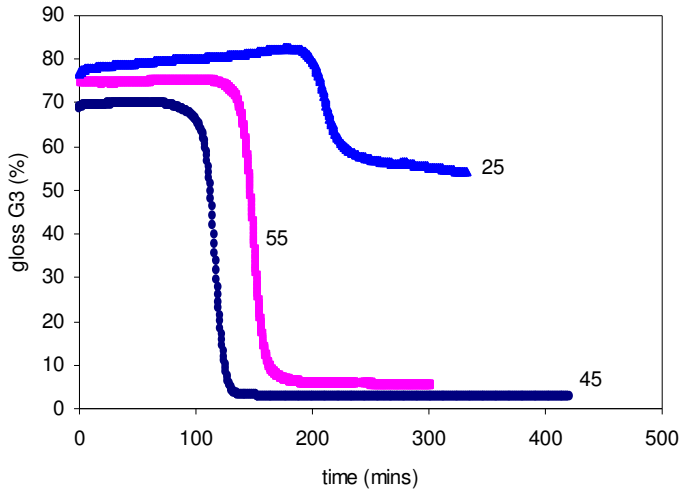

Figure 2a Surfoptic gloss at 3° acceptance angle versus time

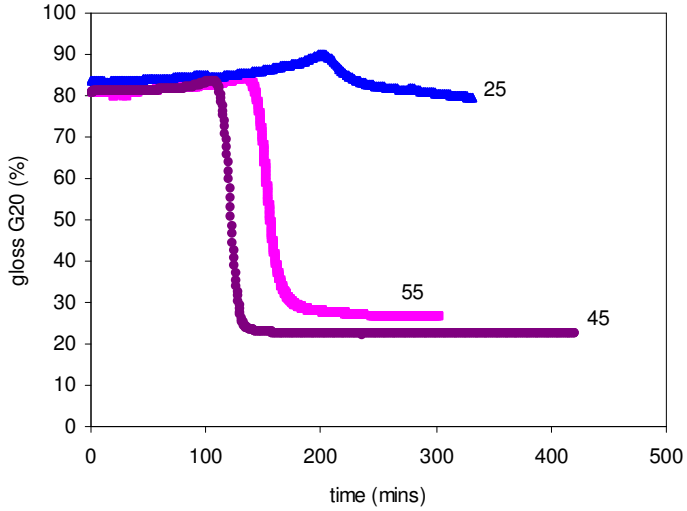

Figure 2b Surfoptic gloss at 20° acceptance angle versus time

The differences in G3 and G20 relate to the angular distribution of the light scattered by the surface, in particular, to the relative amounts of specular, directional-diffuse and diffuse scatter they detect. A schematic for the scattering behaviour is shown in figure 3. G20 is always higher than G3 owing to the contributions of diffuse and directional diffuse scatter. More interesting in figure 2 is the difference around the FCC where G20 shows a distinct peak, but G3 just a smooth shoulder: this difference suggests evolution of structure at the FCC (for all the PVC levels) that creates wider-angle scattering – i.e. light is scattered away from the specular direction into angles between 3° and 20°. This point is revisited below in section 3.3.

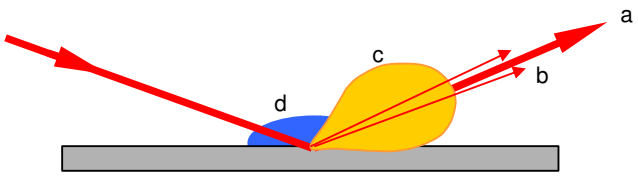

Figure 3. Schematic of scattering at the paint surface. The surface is microrough, but macroscopically flat. Some of the incident beam is reflected specularly (a) and some as a directional-diffuse lobe (c). Some light is refracted into the bulk and undergoes multiple scattering and re-emerges as truly diffuse scatter (d). Relatively large, but infrequent surface irregularities (such as particle aggregates or bubbles) may lead to some reflection at other angles (b)

3.2 Refractive index and microroughness

Figures 4a and b show how the refractive index and microroughness change during drying. All of the films show a significant rise in refractive index up to the FCC. The starting refractive index is close to that of water and the change is consistent with compositional changes as the water evaporates and the binder-pigment concentration increases. Microroughness is very low and remains constant up to the FCC, as would be expected for a surface flattened by surface tension. At the FCC, microroughness increases very rapidly, while refractive index decreases. The development of surface microroughness arises as the pigment particles begin to distort the surface. The refractive index is sensitive to the effective composition of the rough layer, which is (from the point of view of the reflected light) a mixture of air and paint. Therefore the behaviour of refractive index and microroughness is strongly correlated during the transition immediately after the FCC (see Elton and Legrix 2008 for more information on the relation between refractive index and microroughness). The changes in both refractive index and microroughness end rather abruptly for the film formulated at the CPVC, but relatively more slowly for the other PVC levels. Small changes continue at relatively long times.

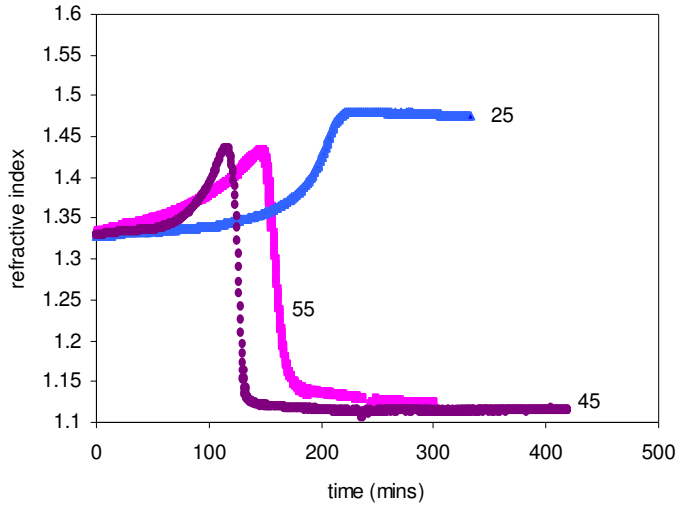

Figure 4a Refractive index versus time

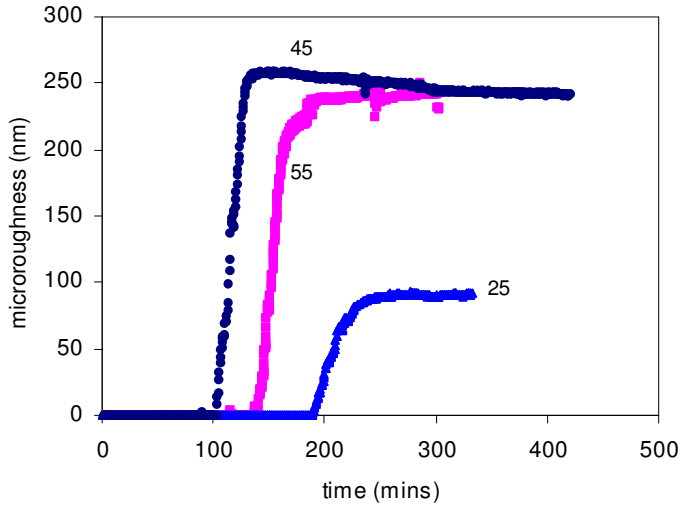

Figure 4b Microroughness versus time

The direct measurements of refractive index and microroughness confirm the main changes inferred from the gloss curves. It can be helpful to look at the correlation between refractive index and microroughness to help understand the relation between the two parameters and changes in the paint film. Correlations are shown in figure 5 and discussed in the figure caption.

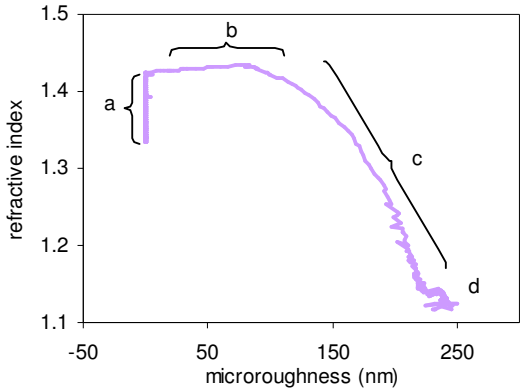

Figure 5a correlation between refractive index and microroughness. Four regions are shown (a) here the paint surface is smooth, but refractive index increases as the pigment concentration increases; (b) refractive index is fairly constant while microroughness begins to increase – here the effect of increasing pigment concentration is balanced by the reduction in refractive index due to air at the surface; (c) refractive index dominated by microroughness ; (d) clear correlation breaks down as more complex structure develops in the surface, both refractive index and microroughness dependent on particle packing, binder levels and porosity.

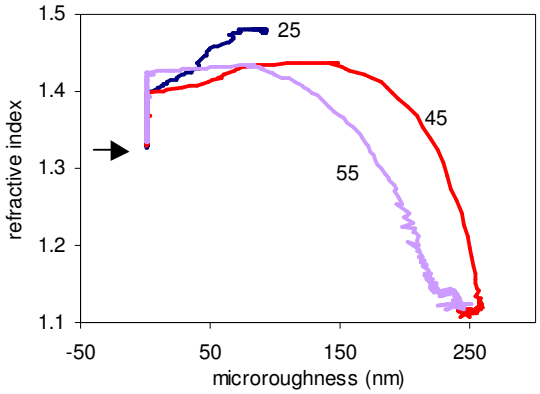

Figure 5b Correlation between refractive index and microroughness for the three PVC levels. The low PVC coating does not get beyond region (b)

3.3 Theoretical gloss

It is quite straightforward to calculate an expected gloss (G_{model}) based on the refractive index and microroughness (Elton 2008). This simple model ignores any contributions from diffuse or directional-diffuse scatter, but the extent to which the predicted trends agree (or disagree) with the observed data can provide insights to structural changes within the coating layer. Model results are compared to the data in figure 6. In principle, in the absence of diffuse, directional diffuse scatter and macroroughness, G3 and G20 should be identical.

The differences between model and observed gloss for the three paints are fairly complicated. It is helpful to consider the time leading up to the FCC and the time after the gloss transition separately. After the gloss transition the differences are fairly consistent at the three PVC levels and $G20 > G_{model} > G3$. G20 is expected to be larger because of the contributions of diffuse and directional diffuse scatter. These effects ought to be more significant above the CPVC and indeed, appear to be so. The fact that $G3 < G_{model}$ is explained by the presence of scattering features in the film which lead to scattering beyond the 3° acceptance angle and which are not accounted for in the model. A similar discrepancy was found for dry films of the same formulations and attributed to the presence of some large-scale roughness features (see Elton and Legrix 2008). However, the discrepancy is very large for the paint at 25% PVC and may be due to a problem in pigment dispersion leading to macrorough features which emerge as the water evaporates and film formation of the binder commences.

Before the FCC, the model gloss varies systematically with PVC relative to the measured glosses:

- 25% PVC $G_{model} < G20$ leading up to the FCC, but are very similar at the FCC.
- 45% PVC $G_{model} \sim G20$ leading up to the FCC, but $G_{model} > G20$ at the FCC.
- 55% PVC $G_{model} > G20$ leading up to the FCC, and at the FCC.

The overestimation of gloss by the model at the FCC increases with PVC, and suggests the evolution of structure around the FCC that causes rather diffuse scattering (outside the nominal ±10° of the G20 detector). For the paint formulated above the CPVC, this diffusely-scattering structure evolves as soon as the paint starts to dry and before the onset of surface microroughness. Visual examination of the dry films suggests a cause for these features – air bubbles. The hand draw-downs suffered from this defect which appeared significantly worse at higher PVC. Air bubbles may tend to emerge from the surface as the water evaporates. Such features would have a significant effect on gloss leading to scattering at very wide angles.

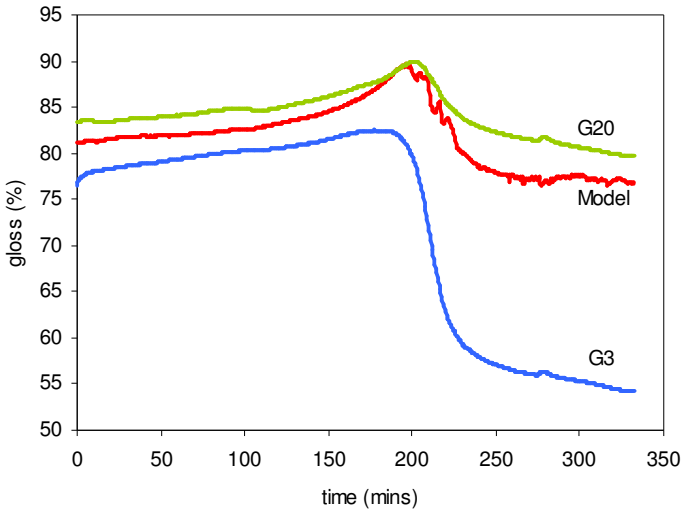

Figure 6a model gloss compared with measured G3 and G20 for 25% PVC film.

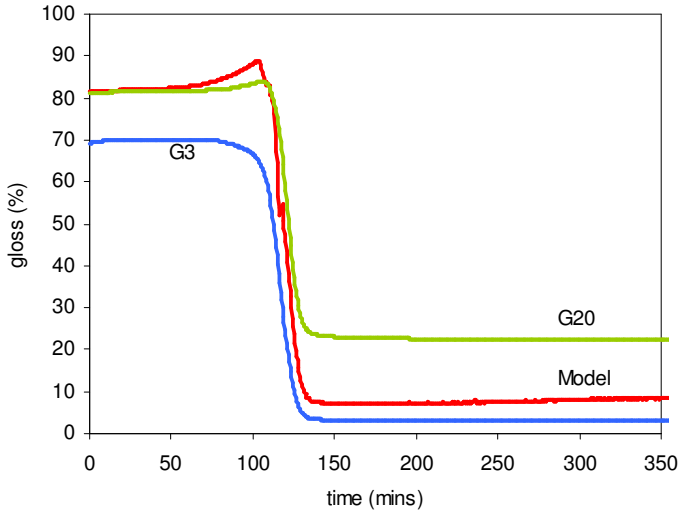

Figure 6b model gloss compared with measured G3 and G20 for 45% PVC film.

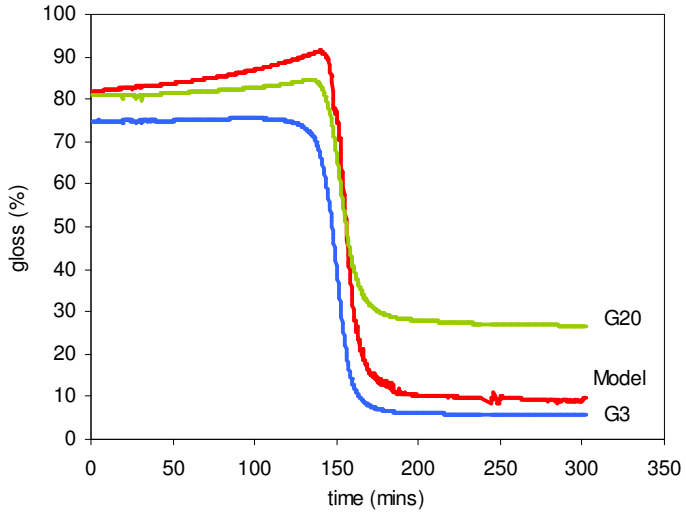

Figure 6c model gloss compared with measured G3 and G20 for 55% PVC film.

3.4 Backscatter

Figures 7a and b shows the backscattered intensity for s- and p-polarised incident light for each of the three paint films as a function of time. Although the incident beams are polarised, the backscattered light is expected to be largely depolarised due to multiple scattering. (The polarisation state of the scattered light is not measured and the labels s and p indicate the state of the incident beam.)

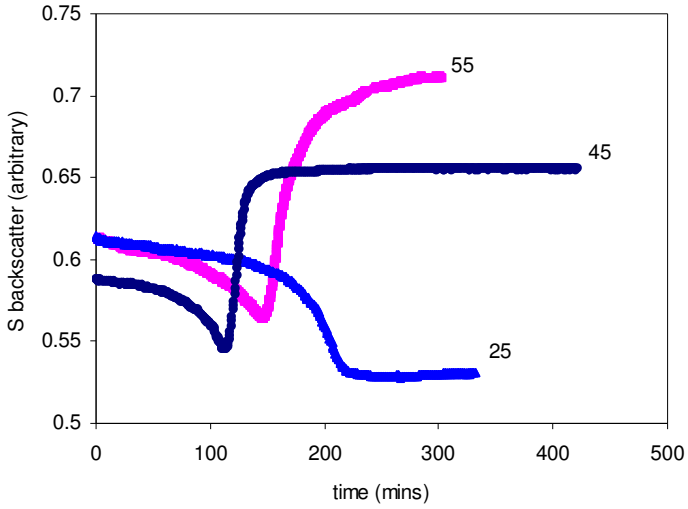

Figure 7a backscattered s-polarised intensity for the three paint films.

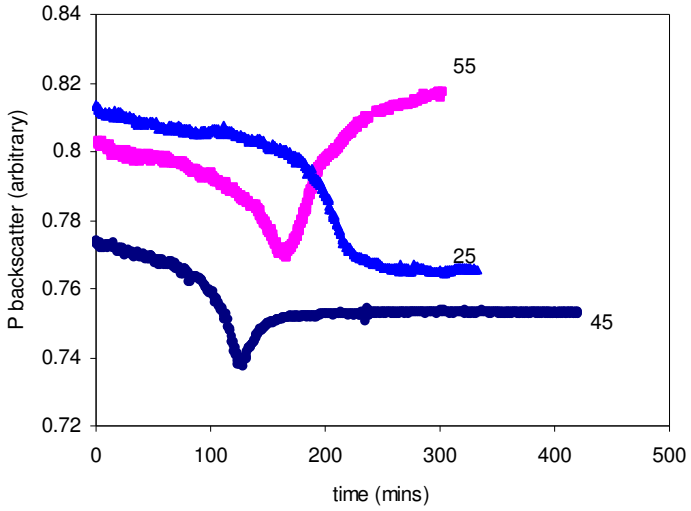

Figure 7b backscattered p-polarised intensity for the three paint films.

The intensity of light backscattered depends on the scattering characteristics of the paint film, but also on the amount of light transmitted into the film. For an incident beam at an oblique angle of incidence, the fraction of light transmitted is polarisation-dependent and controlled by the refractive index. The fraction of light transmitted can easily be calculated from Fresnel's equations and used to correct the measured backscattered intensity for refractive index effects as shown in Appendix II. The resulting corrected backscatter intensity is a measure of scattering in the paint film bulk (although other factors such as the effects of the interface roughness may complicate matters). If scattering is the dominant extinction process in the paint film, the backscatter intensity (B) should be related to the paint film transmittance (T) by B = 1-T, so a minimum in backscatter corresponds to a peak in transmittance and should mark the position in time of the SCC (c.f. figure 1 and figures in Al-Turaif and Lepoutre, 2000). The quantity (1-B) is convenient for plotting and will be called the "inferred transmittance" to clarify that the transmittance is derived rather than measured directly.

Figure 8 shows inferred transmittance (1-B) curves as a function of time for the drying paints, along with the corresponding gloss curves (20° acceptance angle). At 25% PVC, the inferred transmittance rises monotonically to a plateau consistent with a reduction in scattering efficiency due to particle crowding effects. At 45% PVC, the inferred transmittance peaks at the SCC, then falls slightly indicating evolution of some scattering structure. But at 55% PVC – above the CPVC – the inferred transmittance shows a very distinct peak at the SCC and a significant decrease thereafter owing to increased scattering efficiency as air voids begin to be incorporated in the paint film. The changes in gloss with time occur rather quickly between the FCC and SCC, but the changes in scattering are less rapid. Particularly in the case of the 55% PVC paint, significant changes in scattering continue some time after the gloss is fixed, indicating that sub-surface structure continues to evolve after the surface is largely immobilised.

The backscattered intensity is expected to have some relationship to wet opacity.

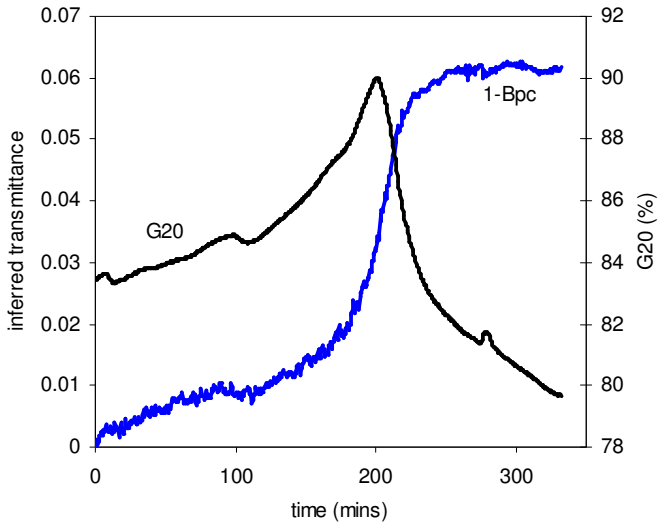

Figure 8a 25% PVC. Inferred transmittance (1-Bpc)and gloss (G20 - 20° acceptance angle) versus time.

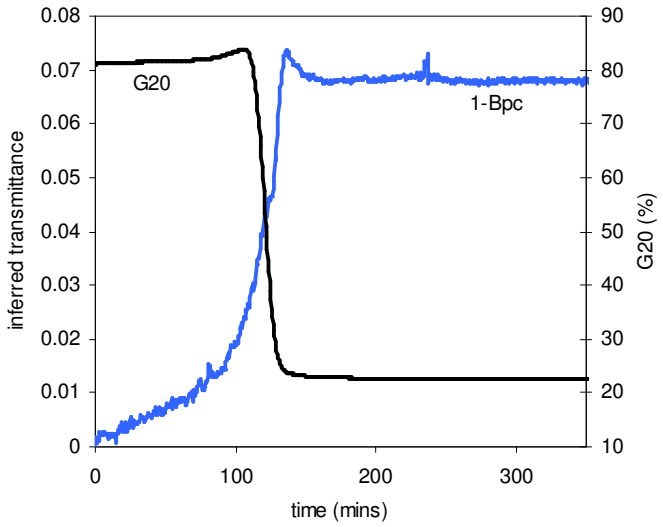

Figure 8b 45% PVC. Inferred transmittance (1-Bpc) and gloss (G20 - 20° acceptance angle) versus time.

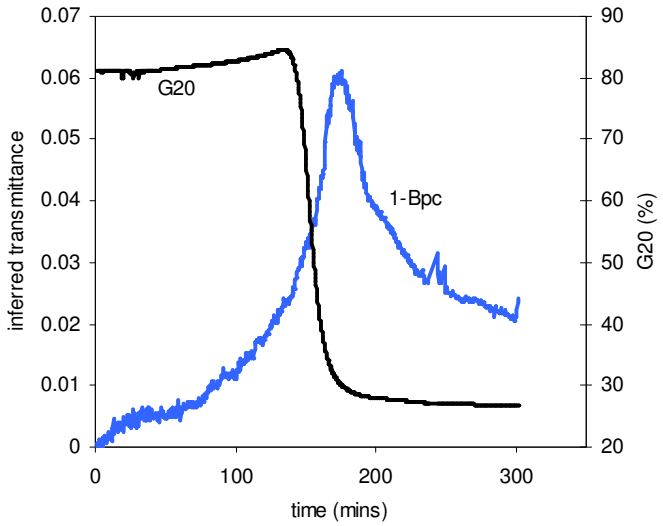

Figure 8c 55% PVC – Inferred transmittance (1-Bpc) and gloss (G20 - 20° acceptance angle) versus time.

Conclusions

Studies of drying paint using gloss measurements (e.g. Al-Turaif and Lepoutre 2000) have inferred the role of refractive index and microroughness. These parameters are measured directly by reflectometry. An expected gloss can be calculated from refractive index and microroughness and compared with measured gloss values. This approach can provide useful insights into the surface structure as deviations between model and observation indicate the existence of other surface-scattering processes. Measurements of gloss at more than one acceptance angle are also useful in this respect. Measurement of the backscattered intensity for polarised incident light can be used to obtain insights into the scattering efficiency of the bulk film. Transmittance data provide similar information, but backscatter measurements have the advantage of being suitable for any substrate. One of the key benefits of reflectometry is the ability to obtain a combination of data (gloss, refractive index, roughness and backscatter) in a each measurement: these data provide a comprehensive picture of the surface and bulk changes during drying.

For the model paints studied here, clear differences are evident in drying behaviour and structure evolution as a function of PVC. The findings are broadly in agreement with previous published studies and confirm an initial increase in refractive index as water evaporates from the paint film reaching a maximum at the so-called first critical concentration (FCC). For films near or above the CPVC, after the FCC the gloss and refractive index fall rapidly as microroughness increases due to the formation of menisci around pigment particles at the surface. These changes in refractive index and microroughness largely explain the observed rapid decrease in gloss. Changes in scattering efficiency within the film generally occur more slowly than, and lag behind, the changes at the surface.

Acknowledgements

Thanks are due to Michèle Julian for preparation of the paint samples.

References

Al-Turaif H and Lepoutre P 2000 Evolution of surface structure and chemistry of pigmented coatings during drying. *Prog. Org. Coat.* **38** 43–52

Braun J H 1991 Gloss of paint films and the mechanism of pigment involvement. *J. Coat. Tech.* **63**, 43-51.

Elton N J 2008 A two-scale roughness model for the gloss of coated paper. *J. Opt. A: Pure Appl. Opt.* **10** 085002

Elton N J and Legrix A 2008 Gloss and surface structure through a paint PVC ladder. Surfoptic Applications Note No. 8 (AN8, Sept 2008)

Gate L F & Preston J S 1995 The specular reflection and surface-structure of emulsion paint films. *JOCCA-Surface Coatings International* **78** (8) 321-330

Further Information

For further information about the Imaging Reflectometer technology or applications, visit www.surfoptic.com or contact Surfoptic at info@surfoptic.com.

Appendix I Simplified paint formulations

Ingredient	PVC 25%	45%	55%
TiO_2 pigment	22.35	21.03	21.03
Kaolin pigment	3.54	13.34	13.34
Dispersants & biocide	0.89	1.10	1.10
Water	22.41	25.24	25.24
Vinyl Acetate Ethylene binder	50.81	39.29	39.29
Total	100.00	100.00	100.00

Appendix II Backscattered light and relation to refractive index

Light incident on a paint film at an oblique angle will be both reflected and refracted. The refracted beam will generally undergo multiple scattering by interactions with pigment particles in the bulk of the paint film. Some of the multiply-scattered light will re-emerge from the top surface as backscatter (Figure A1). The scattering efficiency of the paint can be an important factor in opacity, especially for white paints where absorption may be low. Measurement of backscattered intensity should provide a measure of scattering efficiency. However, the backscatter intensity depends on how much light is refracted into the paint film which in turn depends on the refractive index and it is necessary to correct for the effect.

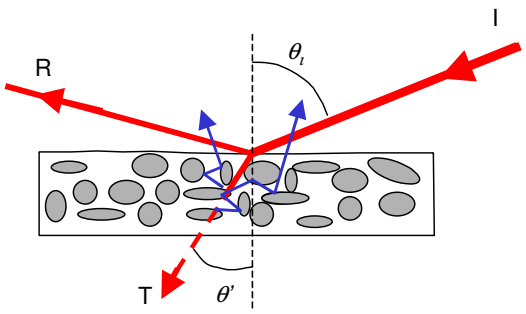

Figure A1
Light incident on the paint film at an oblique angle of incidence (I) is reflected (R) and refracted at the interface between the paint and air. If the paint were transparent (e.g. a varnish), the refracted beam would be transmitted (T). But real paints are heavily pigmented and the refracted beam will generally undergo multiple scattering by pigment particles within the film – some may be absorbed and some eventually transmitted. A fraction of the multiply-scattered light will re-emerge from the top surface (the backscattered light).

In the case of the reflectance of light from a perfectly smooth, homogeneous, isotropic and non-absorbing substrate the fraction of incident power reflected (R) and transmitted (T) is described by Fresnel's equations for s and p polarised light:

$$Rs = \frac{\sin^2(\theta_i - \theta')}{\sin^2(\theta_i + \theta')} \qquad Ts = 1\text{-}Rs \qquad (1)$$

$$Rp = \frac{\tan^2(\theta_i - \theta')}{\tan^2(\theta_i + \theta')} \qquad Tp = 1\text{-}Rp \qquad (2)$$

Where θ' is the angle of refraction,

$$\theta' = \sin^{-1}\left(\frac{n_1 \sin\theta_i}{n_2}\right) \qquad (3)$$

and n_1 and n_2 are the refractive indices of the media on the reflected and refracted side of the interface and θ_i is the angle of incidence.

The intensity of light backscattered by the paint (denoted Bp and Bs for an incident beam having p- and s-polarisation respectively) will be proportional to the intensity in the refracted beam. The effective refractive index is measured by the reflectometer, therefore it is straightforward to calculate *Ts* and *Tp* from (1) and (2). To remove the influence of refractive index from the backscatter intensity it is simply necessary to divide by *Tp* or *Ts* as appropriate to obtain corrected backscatter intensities:

Bpc = Bp/Tp
Bsc = Bs/Ts

The intensity of the refracted beam for incident p-polarised light is rather less influenced by refractive index than the s-polarised beam (Figure A2), and use of *Bpc* is therefore recommended to minimise compounding of errors.

In the absence of significant absorption, the quantity (1 - *Bpc*) is a measure of transmittance.

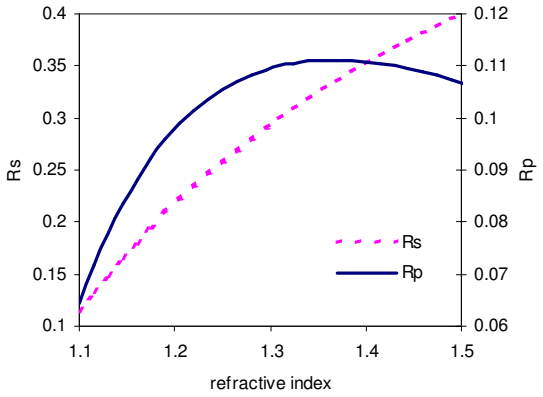

Figure A2
Rs and Rp versus refractive index over the range 1.1 – 1.5 commonly measured in paint films.